Tetrahedron 64 (2008) 8279–8286

Contents lists available at ScienceDirect

Tetrahedron

journal homepage: www.elsevier.com/locate/tet

Rotaxanes with a calix[6]arene wheel and axles of different length. Synthesis, characterization, and photophysical and electrochemical properties

Arturo Arduini [a,*], Rocco Bussolati [a], Alberto Credi [b,*], Andrea Pochini [a], Andrea Secchi [a], Serena Silvi [b], Margherita Venturi [b,*]

[a] Dipartimento di Chimica Organica e Industriale, Università di Parma, via G.P. Usberti 17/A, 43100 Parma, Italy
[b] Dipartimento di Chimica 'G. Ciamician', Università di Bologna, via Selmi 2, 40126 Bologna, Italy

ARTICLE INFO

Article history:
Received 14 March 2008
Received in revised form 20 May 2008
Accepted 30 May 2008
Available online 5 June 2008

Keywords:
4,4′-Bipyridinium
Electrochemistry
Molecular machine
Photochemistry
Supramolecular chemistry

ABSTRACT

We have synthesized a series of three rotaxanes constituted of a calix[6]arene wheel and a 4,4′-bipyridinium unit on the axle, which differ in the length of the two aliphatic chains that connect the central bipyridinium unit with the two terminal stoppers. We have investigated the photophysical and electrochemical properties of these systems and of suitable model compounds in two prototypical solvents, namely, acetonitrile and methylene chloride. Our results show that these rotaxanes are characterized by a complex pattern of intercomponent interactions whose strength can be influenced by the length of the axle as well as the nature of the solvent.

1. Introduction

The functioning of new molecular devices, able to perform programmed tasks, is directly connected with the chemical properties of the fragments or components that constitute their skeleton. This concept is particularly important in those cases in which these devices should respond to external stimuli and work as molecular machines.[1–3] Rotaxanes[4]—namely, interlocked chemical species wherein a macrocyclic (wheel) component encircles a dumbbell-shaped molecule (Fig. 1)—are indeed appealing systems for the construction of artificial molecular machines, because:

- the mechanical bond allows a large variety of mutual arrangements of the molecular components, while conferring stability to the system;
- the interlocked architecture limits the amplitude of the intercomponent motion in the three directions;
- the stability of a specific arrangement (co-conformation)[5] is determined by the strength of the non-covalent intercomponent interactions, which are also responsible for the efficient template-directed syntheses of rotaxanes;
- such interactions can be modulated by external stimulation.

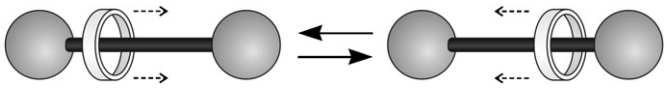

Figure 1. Schematic representation of a rotaxane and of the shuttling motion of its ring component.

Professor Sir Fraser Stoddart, to whom this paper is dedicated, has pioneered the use of molecular recognition and self-assembly processes[6,7] in template-directed protocols for the syntheses of mechanically interlocked compounds such as rotaxanes, catenanes and related species.[5,8–11] His research activity in the past two decades has contributed strongly to the development of the field of molecular devices and machines,[12,13] and is indeed a major source of inspiration for new generations of chemists.[14]

An interesting intercomponent motion that can be envisaged for rotaxanes is the translation—i.e., shuttling—of the wheel component along the axle portion of the dumbbell-shaped component (Fig. 1). In fact, systems of this type, termed molecular shuttles,[15] constitute the most common implementation of the molecular machine concept with rotaxanes.

* Corresponding authors. Tel.: +39 0521 905409; fax: +39 0521 905472 (A.A.); tel.: +39 051 2099543; fax: +39 051 2099456 (A.C. and M.V.).
E-mail addresses: arturo.arduini@unipr.it (A. Arduini), alberto.credi@unibo.it (A. Credi), margherita.venturi@unibo.it (M. Venturi).

0040-4020/$ – see front matter © 2008 Elsevier Ltd. All rights reserved.
doi:10.1016/j.tet.2008.05.123

In order to control the shuttling motion, rotaxanes are usually equipped with two distinct recognition sites ('stations') on their axle portion, which can bind the wheel component to different extents.[16–23] The wheel resides initially on the station that gives the strongest interaction, but can be induced to shuttle onto the other station with an appropriate stimulus that, for instance, weakens the former interaction.

In this work we aim at investigating a different aspect of these systems, that is, the effect of the axle length on the physicochemical properties and dynamic behaviour of one-station rotaxanes. To this purpose, we have designed and synthesized a series of three rotaxanes (**1**–**3**, tosylate salts, Chart 1) bearing a tris(*N*-phenylureido)-calix[6]arene wheel and a 4,4′-bipyridinium station on the axle that differ in the length of the two stoppered aliphatic chains attached to the central bipyridinium unit.

We have recently demonstrated that the triphenylureido calix[6]arene derivatives such as **4** (Chart 1) can act as dissymmetrical three-dimensional heteropolytopic receptors that forms oriented pseudorotaxanes and rotaxanes with 4,4′-bipyridinium derivatives in apolar solvents.[24–26] These complexes are stabilized by a combination of hydrogen bonds, CH-π and charge-transfer interactions between the π-electron rich cavity and the π-electron poor bipyridinium unit[27] and possibly solvophobic effects. The counteranions of the dicationic bipyridinium unit also participate in the stabilization of the complex through hydrogen bonding interactions with the ureidic groups located on the upper rim of the wheel.

We have shown[28,29] that the photophysical properties of these assemblies differ from those of the separated molecular components. We have also observed[28,29] that both the redox potential of the 4,4′-bipyridinium unit of their thread and the kinetics of these redox processes are substantially influenced by the presence of the calixarene wheel. Therefore, we thought that photophysical and electrochemical investigations are particularly appropriate to gain an insight into how the distance between the station, located in the centre of the axle, and the terminal stoppers can affect the properties of these rotaxanes. Moreover, such experiments should enable

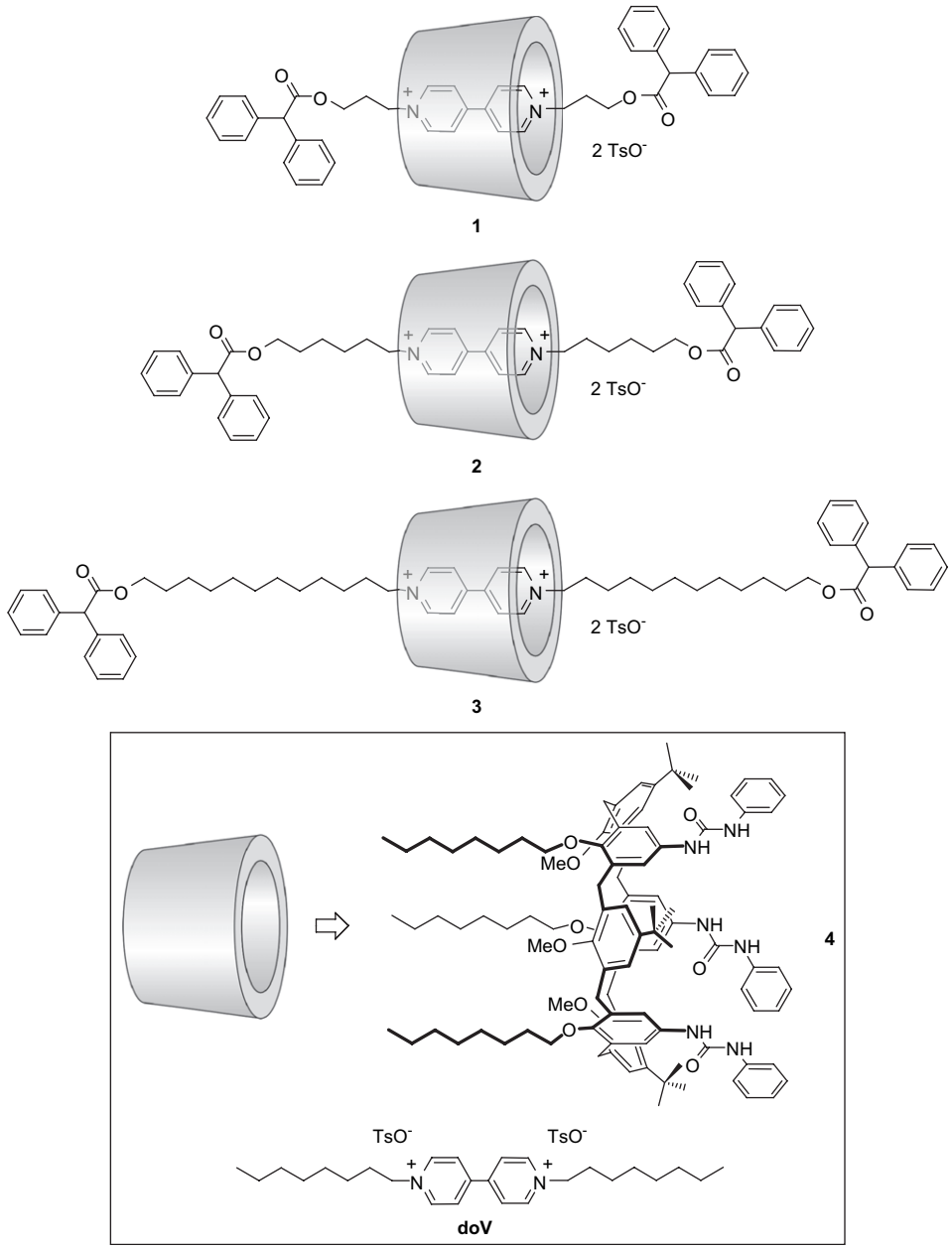

Chart 1. Structural formulae of the examined rotaxanes, of their wheel component **4** and of the 4,4′-bipyridinium model compound **doV**.

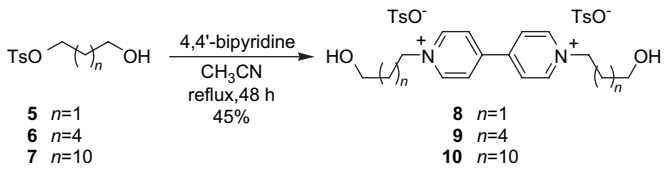

Scheme 1. Synthesis of 4,4′-bipyridinium-based axles bearing alkyl side chains of different length.

us to assess the importance of the various interactions that concur in the stabilization of the system. As the extent of each interaction depends on the nature of the surrounding medium, we chose to study rotaxanes **1**–**3** and their model compounds in two prototypical solvents of different polarity, namely, CH_3CN and CH_2Cl_2.

2. Results and discussion

2.1. Synthesis

Axles **8**–**10** were obtained as tosylate (TsO^-) salts through the synthesis reported in Scheme 1 by refluxing an excess of the corresponding monotosylate (**5**–**7**) with 4,4′-bipyridine in CH_3CN.

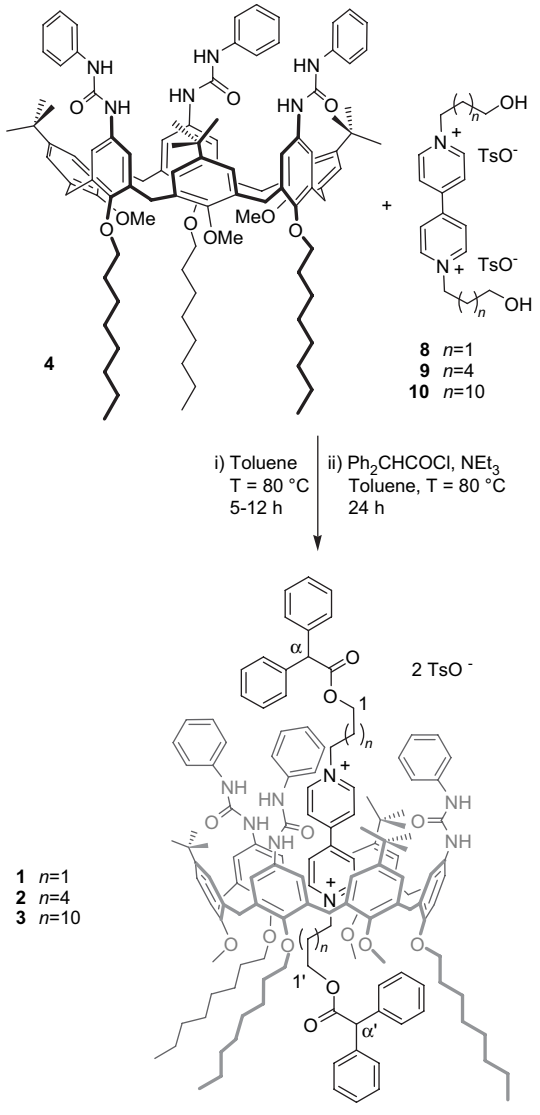

Scheme 2. Template-directed synthesis of rotaxanes **1**–**3**.

Axles **8**–**10** were then used for the synthesis of rotaxanes **1**–**3** (Scheme 2). In a typical experiment the appropriate axle was suspended with an equimolar amount of the calix[6]arene wheel **4** in toluene. To the deep red homogeneous solution that had formed after stirring, an excess of diphenylacetyl chloride and triethylamine were added and the reaction stirred at 80 °C for two days. After column chromatography, rotaxanes **1**–**3** were isolated as tosylate salts in 19, 15 and 10% yield, respectively.

The structure of these rotaxanes was inferred through NMR techniques. The main common feature of the three rotaxanes is that, as expected, the wheel component experiences a conformational rearrangement as a consequence of the threading–stoppering reaction sequence. In fact, as also verified in our previous studies,[24,25] the OCH_3 protons, that in **4** resonate as a broad signal at $\delta \approx 2.9$ ppm, are in all the three rotaxanes **1**–**3** downfield shifted and resonate in the 4.0–3.8 ppm region of the spectrum. This observation indicates that they are no longer oriented inside the calix[6]arene cavity. In addition, the downfield shift of up to 3 ppm experienced by the six NH ureido protons in C_6D_6, CD_2Cl_2 and also in the more polar CD_3CN suggests their participation in hydrogen bonding interactions with the two tosylate anions. On the other hand, the length of the two alkyl chains, that span the dication unit from the two stoppers in the three rotaxanes, considerably influences the resonances of several protons of the dumbbell component. In fact, the methine protons (α and α′) of the two diphenylacetyl stoppers and the O–CH_2 protons (1 and 1′) of the two alkyl chains are in fact no longer magnetically equivalent, because they experience a different magnetic environment due to the intrinsic dissymmetrical geometry of the calixarene wheel. The α proton, being located over the wheel cavity (see Scheme 2 and Fig. 2), undergoes an anisotropic aromatic shielding effect and it resonates at higher field than proton α′.[24–26] In C_6D_6 the α and α′ protons of **1**, characterized by the shortest alkyl spacers, resonate at δ=5.56 and 5.43 ppm, respectively (Fig. 2a). As the length of alkyl spacers is increased the difference of chemical shift ($\Delta\delta$) between the two methine protons tends to decrease: for **2** it is only 0.1 ppm (Fig. 2b) and for **3** the two signals are almost

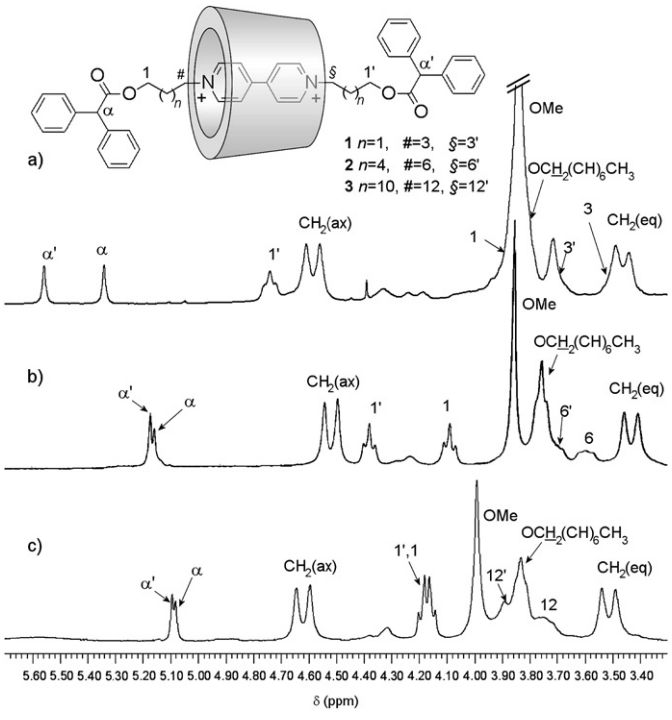

Figure 2. ^1H NMR (expanded region, 300 MHz) spectra of (a) **1**, (b) **2** and (c) **3** taken in C_6D_6 (see drawing for proton labelling of the axles).

Table 1
Absorption (CT band) and electrochemical data of the examined compounds at room temperature

Compound	Solvent: CH_3CN				Solvent: CH_2Cl_2			
	λ_{max} (nm)	ε (M^{-1} cm^{-1})	E_1 (V vs SCE)[a]	E_2 (V vs SCE)[a]	λ_{max} (nm)	ε (M^{-1} cm^{-1})	E_1 (V vs SCE)[a]	E_2 (V vs SCE)[a]
doV			−0.42	−0.86			−0.27	−0.81
1	460[b]	580[b]	−0.59[c]	−1.20[c]	470[b]	510[b]	−0.63[c]	−1.15[c]
2	455	560	−0.62	−1.14	465	550	−0.71[c]	−1.16[c]
3	450	540	−0.62	−1.18	461	590	−0.73[c]	−1.20[c]

[a] Argon-purged solution.
[b] Shoulder on the lower-energy side of an intense absorption band; see Figure 3.
[c] Cyclic voltammogram characterized by a large (>90 mV) peak-to-peak separation; potential value estimated by DPV peaks.

undistinguishable (Fig. 2c). The shielding effect of the calixarene cavity was even more pronounced for the methylene groups 1 and 1′. In **1** the two resonances are separated by almost 1 ppm.

The threading of the axle inside the wheel was also confirmed, in all instances, by the extensive upfield shift experienced by both the aromatic protons of the bipyridinium unit and the protons of the (py)N–CH_2 methylene groups. The chemical shift of the broad signals corresponding to the latter protons (3–3′, 6–6′ and 12–12′ for **1**, **2** and **3**, respectively) is still strictly dependent on the length of the alkyl chains.

2.2. Absorption and luminescence properties

The absorption spectra of the rotaxanes **1**–**3**, of their wheel component **4** and of the tosylate salt of 1,1′-dioctyl-4,4′-bipyridinium (dioctylviologen tosylate, **doV**), selected as a model compound for the 4,4′-bipyridinium unit contained in their axles, have been recorded either in CH_2Cl_2 or in CH_3CN at room temperature. All the spectroscopic data are gathered in Table 1.

For all the rotaxanes the absorption spectra show an intense band with maximum at around 260 nm, attributed to the absorption of the wheel component and the bipyridinium unit contained in the axle components,[28] and a weak and broad band with maximum around 460 nm. This visible band (Fig. 3) can be ascribed to the charge-transfer (CT) interactions between the electron-rich aromatic rings of the wheel and the electron-poor bipyridinium unit contained in the rotaxane axles. Such an assignment is supported by the fact that similar bands appear in the spectra of the pseudorotaxanes formed by mixing in CH_2Cl_2 equimolar amounts of **4** and **doV** or an axle containing a bipyridinium unit and a diphenylacetic group as a stopper.[28]

It is interesting to notice that the visible absorption bands of the examined rotaxanes are very similar as far as energy and intensity are concerned, and are practically unaffected by the nature of the solvent (Table 1 and Fig. 3). The molar absorption coefficient of the CT band (ε_{CT}) can be correlated[30] with the magnitude of the donor–acceptor electron-coupling matrix element (H_{DA}) by Eq. 1, derived from the Hush theory for optical charge transfer:[31,32]

$$\varepsilon_{CT} = \frac{k r_{DA}^2}{E_{CT} \Delta\nu_{CT}^{1/2}} H_{DA}^2 \quad (1)$$

where k is a numeric constant, r_{DA} is the donor–acceptor distance, E_{CT} is the energy of the optical charge-transfer transition (which is related to the λ_{max} of the corresponding CT band) and $\Delta\nu_{CT}$ is the half-width of the CT band. The absorption spectra (Fig. 3) show that E_{CT} and $\Delta\nu_{CT}$ are very similar for all three rotaxanes in the two solvents examined, and it can be expected that r_{DA} is substantially unchanged on going from **1** to **3**. Therefore, we can conclude that the donor–acceptor electronic coupling—and hence the CT interaction—is not much affected by solvent polarity and is essentially the same for all three rotaxanes.

As previously noticed,[28] **doV** does not show any luminescence. The fluorescence typical of the free calixarene **4** (λ_{max}=340 nm) is no longer observed in rotaxanes **1**–**3**. It is very likely that CT interactions are responsible for such a fluorescence quenching, because they introduce new excited states that offer a radiationless deactivation path to the upper lying, potentially luminescent level of wheel **4**.[28,33,34]

Charge-transfer interactions, however, are not the sole intercomponent forces that characterize these compounds. Remarkably, X-ray crystallography in the solid state evidenced[27] that C–H···O hydrogen bonding[35] between some H atoms of the axle and O atoms of the methoxy groups of the wheel takes place. Spectroscopic and electrochemical experiments on pseudorotaxane analogues in CH_2Cl_2 and CH_3CN support these findings: in CH_2Cl_2 wheel **4** and **doV** self-assemble very efficiently (K_a>5×10^5 M^{-1}),

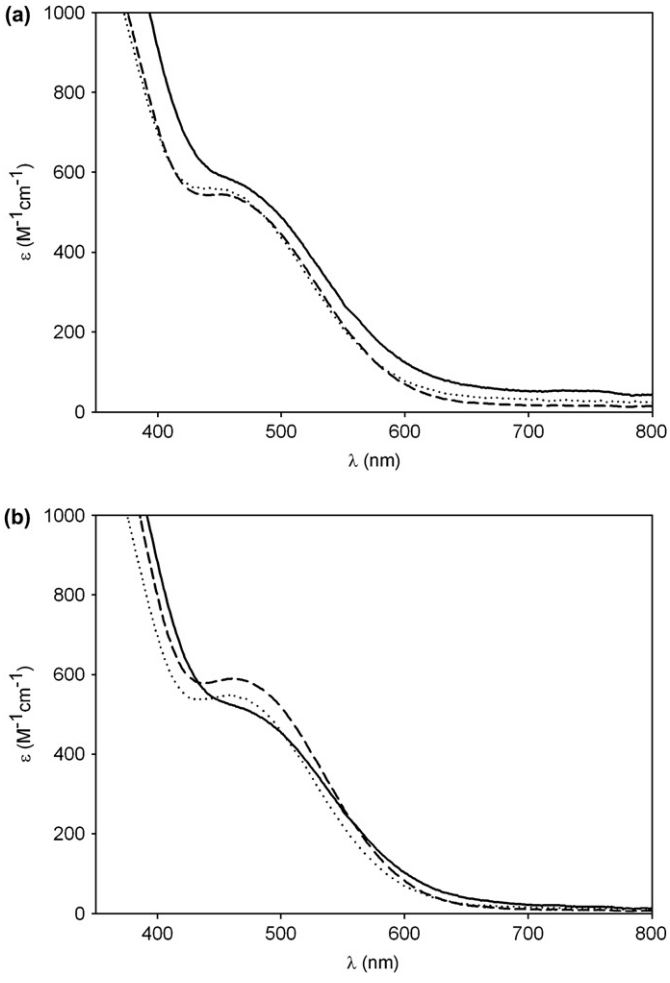

Figure 3. Charge-transfer absorption band of the three rotaxanes in (a) CH_3CN and (b) CH_2Cl_2: **1**, full line; **2**, dotted line; **3**, dashed line.

whereas in the conditions employed for the spectroscopic and electrochemical experiments there is no evidence of association in the more polar CH_3CN solvent. Because hydrogen bonding interactions are stronger in apolar solvents, it may be expected that in CH_2Cl_2 the C–H···O contacts can contribute in a substantial manner to the stabilization of the adduct. Furthermore, in CH_2Cl_2 solvophobic effects should be taken into consideration, because it is well known that methylviologen is insoluble in this solvent and the solubility of **doV** is much lower than in CH_3CN. It may be inferred that the cavity of the calixarene wheel offers to the bipyridinium unit of the axle a more polar environment compared to CH_2Cl_2, thereby favouring its threading into the wheel. Hydrogen bonds, in contrast with CT interactions, do not give rise to new absorption bands in the visible region and affect only very slightly the absorption spectra of the molecular components.[36,37] Hence, absorption spectroscopy does not allow us to evidence such C–H···O interactions.

On the contrary, ^{1}H NMR spectroscopy would be a perfect tool to monitor the occurrence of hydrogen bonds in solution. Unfortunately, in this case the NMR spectroscopic observation of C–H···O bridges between the axial component and the wheel are prevented because of the position assumed by the axle inside the aromatic cavity. In principle, these weak hydrogen bonding interactions should determine a moderate deshielding effect on the proton resonances of the methylene group adjacent to the pyridine ring and oriented towards the calix[6]arene narrow rim (i.e., protons 3′, 6′ and 12′ in **1**, **2** and **3**, respectively; see Fig. 2). However, as we noticed in previous investigations,[24–26] the threading of a viologen-based axle inside the calix[6]arene wheel usually determines a pronounced upfield shift (from 0.6 to 1 ppm, depending on the axle type) of the aforementioned methylene protons, owing to the more intense anisotropic shielding effect exerted by the aromatic nuclei of the macrocycle. Therefore, although it is likely that the C–H···O hydrogen bonds evidenced in the solid state[27] take place in solution as well,[35] they cannot be clearly detected from the NMR spectra.

2.3. Electrochemical properties

The electrochemical investigations have been performed by cyclic voltammetry (CV) and differential pulse voltammetry (DPV) on the tosylate salts of rotaxanes **1**–**3** and the model compound **doV** at room temperature in argon-purged CH_2Cl_2 and CH_3CN; the results obtained are gathered in Table 1 and Figure 4.

The model compound **doV** shows two reversible and monoelectronic reduction processes typical of bipyridinium-based compounds[38,39] that occur at potential values less negative in CH_2Cl_2 than in CH_3CN. This observation can be unequivocally attributed to the fact that, in the apolar CH_2Cl_2 solvent, less charged or uncharged species are better stabilized than in the more polar CH_3CN. Therefore the dicationic bipyridinium unit is more easily reduced in CH_2Cl_2 than in CH_3CN. As expected for an effect related to charge, the potential difference between the two solvents is more pronounced for the first reduction process than for the second one (Table 1 and Fig. 4).

All three rotaxanes **1**–**3** exhibit two monoelectronic chemically reversible reduction processes that can be assigned to the bipyridinium unit contained in their axle component (see, e.g., Fig. 5), and also exhibit chemically irreversible oxidation processes characteristic of their calixarene-based wheel component.[28] These latter processes, being irreversible and not of fundamental importance in the context of the present paper, will not be discussed.

First of all, the chemical reversibility observed for the reduction processes of compounds **1**–**3** suggests that either no chemical rearrangement is associated to the redox processes or such a rearrangement is fast on the time scale of the electrochemical scan.[40,41]

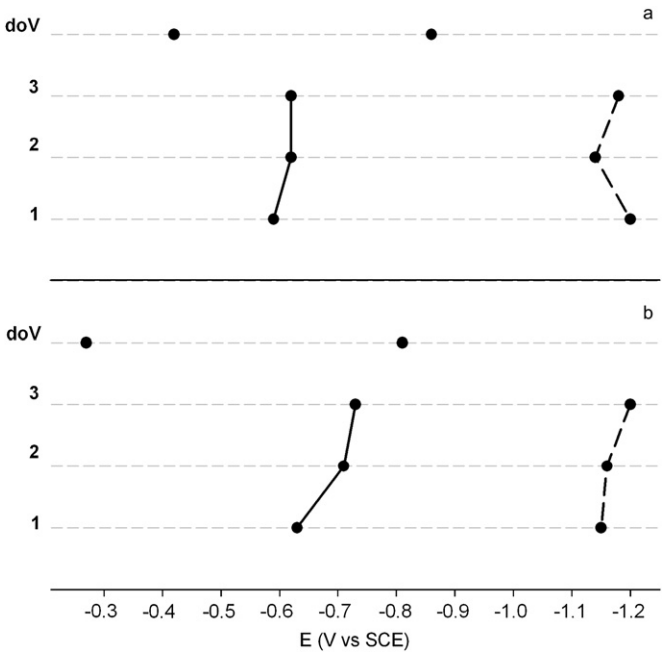

Figure 4. Genetic diagram for the first (full line) and second (dashed line) reduction processes of the model compound **doV** and the three rotaxanes in (a) CH_3CN and (b) CH_2Cl_2.

As we will discuss later on, the potential values are in better agreement with the first hypothesis. In CH_2Cl_2 all the CV waves show some degree of electrochemical irreversibility with peak-to-peak separations in the order of 150–200 mV at a scan rate of 200 mV s^{-1} (see, e.g., Fig. 5). These results are consistent with the behaviour of the pseudorotaxane assembled from **doV** and **4**, and can be explained considering that the encapsulation[42,43] of the electroactive bipyridinium unit inside the calixarene slows down the heterogeneous electron-transfer kinetics.[28] On the contrary, in CH_3CN only the CV waves of rotaxane **1** exhibit a peak-to-peak separation larger than that expected[40] for an electrochemically reversible process. This observation suggests that in the case of the shorter-tethered rotaxane **1** the redox-active bipyridinium unit is more effectively confined inside the cavity of the wheel, most likely because of the close proximity of the two stoppers.

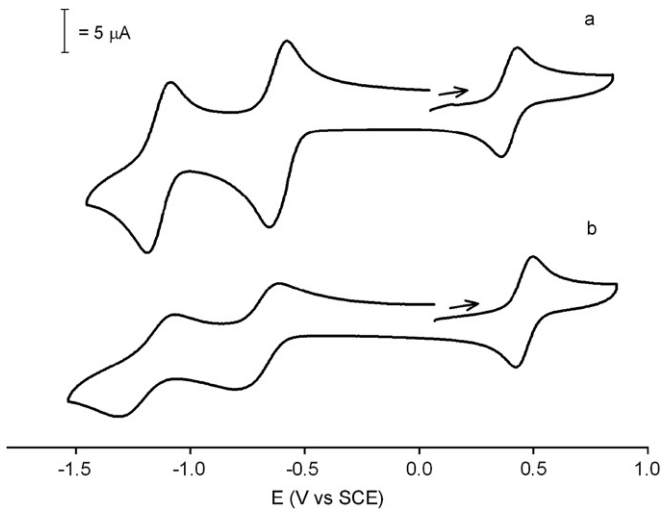

Figure 5. Cyclic voltammograms of compound **2** in Ar-purged (a) CH_3CN and (b) CH_2Cl_2. Concentration, 0.5 mM; scan rate, 200 mV s^{-1}. The wave in the region of positive potentials is that of ferrocene used as a standard.

As shown in Table 1 and Figure 4, the two reduction processes of the three rotaxanes are shifted towards more negative potential values in comparison with the corresponding processes of the **doV** model compound, both in CH_3CN and CH_2Cl_2. The shift of the first reduction can be attributed to the interactions with the wheel that, increasing the electron density on the bipyridinium unit, makes its reduction more difficult. The shift of the second reduction process indicates that when the bipyridinium unit is in the monoreduced form, some interactions remain between the axle component and the wheel. A similar behaviour has been observed for other bipyridinium-containing rotaxanes.[44–46] When the axle is a radical cation, the interactions responsible for the stabilization of the adduct are weaker, but the monoreduced bipyridinium is still an electron acceptor. Such a weak interaction can be established because of the presence of the stoppers that force the bipyridinium unit to stay near the wheel. It has indeed been observed[28,29] that, in related pseudorotaxane systems, one-electron reduction causes dethreading of the molecular components. In rotaxanes **2** and **3** the long side chains (6 and 12 methylene units, respectively) would enable the shuttling of the wheel far from the monoreduced bipyridinium unit. The fact that the second reduction potential is negatively shifted with respect to the free axle also in these species means that the residual CT interaction is strong enough to keep the wheel close to the bipyridinium station. Further support for this conclusion stems from the electrochemical irreversibility exhibited by the second reduction process, indicating that the monoreduced bipyridinium unit is still included in the wheel and hence partially shielded from the electrode.[42,43]

In the first instance, we take into account the effect of the length of the chain and we compare the three rotaxanes in each solvent. We will limit the following discussion to the first reduction process because the changes in the potential value for the second reduction process on going from **1** to **3** cannot be easily rationalized on the basis of the data available for these rotaxanes. We observe that, both in CH_3CN and CH_2Cl_2 solution, the first reduction process for rotaxane **1** is shifted to less negative potential (around 30 and 100 mV, respectively) with respect to rotaxanes **2** and **3**, which show, on the other hand, comparable reduction values.

Such an observation implies that the rotaxanes with longer chains are more difficult to reduce than the rotaxane with the short chain. In other words, both rotaxanes **2** and **3** are more stable than **1** in their dicationic form. The charge-transfer interactions between the axle and the wheel are similar in the three rotaxanes because the CT bands in the absorption spectra have the same energy and intensity (see absorption and luminescence properties). Hence, the different behaviour of **1** compared to **2** and **3** could be related to the other main intercomponent interactions, i.e., hydrogen bonds: the axle of compound **1** is so short that it could not be able to make efficient C–H···O contacts with the wheel. The fact that the potential shift of **1** with respect to the longer-chain rotaxanes is more pronounced in CH_2Cl_2 than in CH_3CN could be explained considering that in the latter solvent the hydrogen bonding interactions are less favoured.

A concomitant—or even alternative—explanation for this behaviour is that the shortness of the axle would force rotaxane **1** to be more deeply encapsulated inside the cavity of the wheel. As a consequence of this constraint, the axle could assume a structure in which the dihedral angle between the two pyridinium rings is lower than in the case of rotaxanes **2** and **3**. It is indeed known[47] that in bipyridinium-type compounds the first reduction potential decreases by increasing the planarity of the aromatic rings, which favours electron delocalization.[38] Therefore, steric constraints may also be responsible for the surprisingly low first reduction potential of **1**.

Additionally, if we compare the three rotaxanes in the two solvents, we can observe that: (i) the first reduction process for rotaxane **1** takes place at nearly the same value in both solvents and (ii) in CH_3CN rotaxanes **2** and **3** are easier to reduce than in CH_2Cl_2.

The negligible solvent effect on the first reduction potential observed for rotaxane **1** [point (i)], in spite of the remarkable solvent dependence of the potential for the analogous process in **doV** (Table 1 and Fig. 4), can be ascribed to the fact that the bipyridinium unit, being deeply encapsulated within the wheel–stoppers ensemble, would experience only the environment created by the interior of the calixarene.

On the contrary, the first reduction potentials of rotaxanes with a longer chain are affected by the nature of the solvent [point (ii)]: in particular, the reduction of compounds **2** and **3** is more difficult in the less polar CH_2Cl_2 (ΔE_1 ca. 100 mV). When the chain of the axle is longer, the bipyridinium unit is not shielded from the solvent like in rotaxane **1**, and moreover the axle can optimize all the stabilizing interactions. If we compare the rotaxanes **2** and **3** with the model compound **doV**, we would expect a similar behaviour in the two solvents: in CH_3CN the charged, oxidized species, are more stable than in CH_2Cl_2, therefore the dicationic rotaxanes should be more easily reduced in CH_2Cl_2 than in CH_3CN. However, compounds **2** and **3** exhibit an opposite behaviour compared to the free axle. To explain this difference we have to again take into account the interactions that stabilize the rotaxanes. As already pointed out, the CT interactions between the molecular components give the same contributions in all the rotaxanes, in both solvents, and so they do not explain this different behaviour. Also in this case, solvent-dependent hydrogen bonding interactions need to be invoked for the further stabilization of the rotaxanes **2** and **3** in CH_2Cl_2.

3. Conclusion

We have designed and synthesized a series of one-station rotaxanes made of a calixarene wheel and three bipyridinium-based axles of different lengths. We have studied their spectroscopic and electrochemical properties in two solvents in order to investigate the effect of the chain length and of the polarity of the solvent on the physico-chemical properties and dynamic behaviour of the rotaxanes. The results demonstrate that these interlocked species are characterized by a variety of intercomponent stabilizing interactions that affect the spectroscopic and electrochemical properties of the systems, and that can be tuned changing the polarity of the solvent. Compound **1** shows the most peculiar behaviour: because of its short axle, the central bipyridinium unit appears to be completely encapsulated in the cavity of the calixarene, and its properties no longer depend on the solvent.

This investigation also emphasizes the potentialities of the techniques employed to estimate the nature and the strength of the various kinds of interactions that can take place between the molecular components in supramolecular systems. In particular, electrochemical measurements are a powerful tool to highlight weak interactions, which usually do not give rise to appreciable changes in the absorption and luminescence spectra.

4. Experimental section

4.1. Synthesis

4.1.1. General remarks

All reactions were carried out under nitrogen; all solvents were freshly distilled under nitrogen and stored over molecular sieves for at least 3 h prior to use. All other reagents were of reagent grade quality as obtained from commercial suppliers and were used without further purification. Column chromatography was performed on silica gel 63–200 mesh. Melting points are uncorrected.

Elemental analyses were carried out at the laboratory of microanalysis of Dipartimento Farmaceutico of the University of Parma. Calix[6]arene (**4**),[48] 3-hydroxypropyl 4-methylbenzenesulfonate (**5**),[49] 6-hydroxyhexyl 4-methylbenzenesulfonate (**6**)[50] and 12-hydroxydodecyl 4-methylbenzenesulfonate (**7**)[51] were synthesized according to the literature procedures.

*4.1.2. General procedure for the synthesis of axles **8**–**10***

A solution of the appropriate tosylate (**5**–**7**, 6.5 mmol) and 4,4′-bipyridine (0.4 g, 2.6 mmol) in CH_3CN (300 ml) was stirred under reflux for 48 h. Afterwards, the solution was evaporated to dryness under reduced pressure.

*4.1.2.1. 1,1′-Bis(3-hydroxypropyl)-4,4′-bipyridine-1,1′-diium ditosylate (**8**).* The oily residue was washed with few portions of acetonitrile to afford **8** (tosylate salt) as a pale greenish oil (45%). ^{1}H NMR (CD_3OD, 300 MHz): δ 9.19 (4H, d, J=6.7 Hz), 8.57 (4H, d, J=6.7 Hz), 7.64 (4H, d, J=8.1 Hz), 7.19 (4H, d, J=8.1 Hz), 4.82 (4H, t, J=7.0 Hz), 3.64 (4H, br t), 2.32 (6H, s), 2.22 (2H, t, J=6.3 Hz); ^{13}C NMR (CD_3OD, 75 MHz): δ 151.8, 148.1, 146.0, 144.6, 142.5, 130.8, 129.2, 128.8, 128.7, 127.7, 127.6, 61.7, 59.8, 35.3, 22.1; IR (KBr): $\tilde{\nu}$ 3388 (s), 3020 (w), 2927 (w), 2890 (w), 1639 (m), 1450 (w), 1215 (m), 1186 (m), 1123 (m), 1035 (m), 1011 (w), 816 (w), 685 (w). Anal. Calcd for $C_{30}H_{36}N_2O_8S_2$: C, 58.42; H, 5.88; N, 4.54; S, 10.40. Found: C, 58.51; H, 5.95; N, 4.87; S, 10.15; ESI-MS (m/z): 273 $[M-H]^+$.

*4.1.2.2. 1,1′-Bis(6-hydroxyhexyl)-4,4′-bipyridine-1,1′-diium ditosylate (**9**).* The oily residue was triturated with acetonitrile to afford **9** (tosylate salt) as a white solid (50%). ^{1}H NMR (CD_3OD, 300 MHz): δ 9.22 (4H, d, J=6.8 Hz), 8.62 (4H, d, J=6.8 Hz), 7.65 (4H, d, J=8.1 Hz), 7.21 (4H, d, J=8.1 Hz), 4.71 (4H, t, J=7.6 Hz), 3.54 (4H, t, J=6 Hz), 2.35 (6H, s), 2.0 (4H, br t), 1.6–1.4 (12H, m); ^{13}C NMR (CD_3OD, 75 MHz): δ 151.8, 147.3, 143.9, 142.0, 130.2, 128.6, 127.2, 63.5, 62.9, 33.5, 32.8, 27.3, 26.7, 21.6; IR (KBr): $\tilde{\nu}$ 3430 (s), 3070 (w), 3052 (w), 2937 (w), 2860 (w), 1641 (m), 1447 (w), 1206 (s), 1204 (s), 1123 (m), 1035 (m), 1011 (w), 819 (w), 685 (w). Anal. Calcd for $C_{36}H_{48}N_2O_8S_2$: C, 61.69; H, 6.90; N, 4.00; S, 9.15. Found: C, 61.81; H, 6.95; N, 4.18; S, 8.96; ESI-MS (m/z): 357 $[M-H]^+$; mp: 112.5–113.5 °C.

*4.1.2.3. 1,1′-Bis(12-hydroxydodecyl)-4,4′-bipyridine-1,1′-diium ditosylate (**10**).* The oily residue was triturated with acetonitrile to afford **10** (tosylate salt) as a white sticky solid. ^{1}H NMR (DMSO-d_6, 300 MHz): δ 9.36 (4H, d, J=6.4 Hz), 8.76 (4H, d, J=6.4 Hz), 7.49 (4H, d, J=7.8 Hz), 7.11 (4H, d, J=7.8 Hz), 4.68 (4H, t, J=7.2 Hz), 3.36 (4H, t, J=6.3 Hz), 2.28 (6H, s), 1.95 (4H, br t), 1.39 (4H, br t), 1.3–1.1 (24H, m); ^{13}C NMR (DMSO-d_6, 75 MHz): δ 148.3, 145.6, 145.4, 137.5, 127.9, 126.4, 125.3, 117.8, 60.8, 60.4, 32.3, 30.6, 29.0, 28.8, 28.6, 28.2, 25.3, 25.2, 20.5; IR (KBr): $\tilde{\nu}$ 3441 (s), 3125 (w), 3057 (w), 2920 (s), 2850 (s), 1640 (s), 1561 (w), 1507 (w), 1468 (w), 1445 (w), 1220 (s), 1186 (s), 1125 (m), 1044 (m), 1033 (m), 1011 (m), 843 (w), 817 (w), 684 (w). Anal. Calcd for $C_{48}H_{72}N_2O_8S_2$: C, 66.33; H, 8.35; N, 3.22; S, 7.38. Found: C, 66.51; H, 8.40; N, 3.41; S, 7.26; CI-MS (m/z): 525 $[M-H]^+$; mp: 178–180 °C.

*4.1.3. General procedure for the synthesis of rotaxanes **1**–**3***

A suspension of the appropriate axle (**8**–**10**, 0.1 mmol) and calix[6]arene **4** (0.15 g, 0.1 mmol) in toluene (50 ml) was stirred for 5 h at 80 °C. Afterwards, when the mixture turned in a deep red homogeneous solution, diphenylacetyl chloride (0.05 g, 0.2 mmol) and triethylamine (0.02 g, 0.2 mmol) were added. After being stirred for 24 h at 80 °C, the mixture was evaporated to dryness under reduced pressure.

*4.1.3.1. Compound **1**.* The resulting reddish solid residue was purified by column chromatography (CH_2Cl_2/CH_3OH=20:1) to afford **1** (tosylate salt) as red solid compound (19%). ^{1}H NMR (C_6D_6, 300 MHz): δ 9.50 (6H, br s), 8.25 (6H, br s), 8.1–7.9 (10H, m), 7.8–7.6 (16H, m), 7.52 (2H, br d), 7.4–7.2 (3H, m), 7.2–7.0 (18H, m), 6.90 (2H, br d), 6.78 (2H, br d), 6.7–6.6 (4H, br s), 5.56 and 5.34 (2H, 2s), 4.74 (2H, br t), 4.59 (6H, br d), 4.2–3.6 (21H, m), 3.46 (6H, br d), 2.6 (2H, br s), 2.07 (6H, s), 1.97 (6H, br t), 1.9–1.3 (32H, m), 1.05 (9H, br t); ^{13}C NMR (C_6D_6, 75 MHz): δ 172.5, 172.0, 153.6, 153.2, 149.6, 148.6 (2 resonances), 147.7, 146.7, 144.9, 143.6, 143.4, 141.4, 139.8, 139.4, 139.3, 137.7, 134.0, 133.0, 132.4, 129.6, 129.4, 129.1, 129.0, 128.9, 128.7, 127.5, 127.3, 126.8, 126.5, 126.1, 125.5, 121.5, 118.4, 116.9, 73.5, 72.0, 69.6, 67.5, 65.6, 64.0, 61.5, 61.0, 59.2, 58.8, 57.3, 34.9, 32.7, 31.8, 31.2, 30.9, 30.1, 29.9, 29.7, 29.4, 28.4, 26.7, 23.0, 21.1, 14.3. Anal. Calcd for $C_{160}H_{188}N_8O_{19}S_2$: C, 74.16; H, 7.31; N, 4.32; S, 2.47. Found: C, 73.47; H, 7.44; N, 4.23; S, 2.40; ESI-MS (m/z): 2419 $[\mathbf{1}\cdot TsO]^+$, 1124 $[\mathbf{1}]^{++}$; mp: 103–104 °C.

*4.1.3.2. Compound **2**.* The resulting reddish solid residue was purified by column chromatography (CH_2Cl_2/CH_3OH=20:1) to afford **2** (tosylate salt) as a red solid compound (15%). ^{1}H NMR (C_6D_6, 300 MHz): δ 9.45 (6H, br s), 8.21 (6H, d, J=7.5 Hz), 8.1–7.8 (16H, m), 7.64 (6H, s), 7.48 (6H, d, J=7.5 Hz), 7.3–7.1 (15H, m), 6.95 (6H, d, J=7.5 Hz), 6.9 (2H, br d), 6.8–6.7 (6H, m), 5.17 (1H, s), 5.16 (1H, s), 4.51 (6H, d, J=15 Hz), 4.38 (2H, br t), 4.08 (2H, br t), 3.85 (9H, br s), 3.8–3.7 (8H, m), 3.6 (2H, br t), 3.42 (6H, d, J=15 Hz), 2.1 (2H, br s), 2.00 (6H, s), 1.9–1.3 (77H, m), 0.99 (9H, br t); ^{13}C NMR (C_6D_6, 75 MHz): δ 172.9, 172.8, 154.1, 153.7, 149.2, 148.1, 146.4, 144.6, 143.7, 141.6, 140.0, 139.8, 137.5, 134.6, 132.9, 130.3, 130.2, 129.8, 129.6, 129.5, 129.4, 127.2, 125.7, 125.3, 121.9, 118.2, 117.2, 77.1, 73.6, 65.5, 65.4, 61.4, 60.8, 58.2, 57.5, 53.1, 34.4, 31.8, 31.6, 31.0, 30.7, 30.4, 30.2, 29.7, 29.4, 28.9, 28.5, 28.3, 26.5, 26.0, 25.8, 22.6, 21.3, 14.1; IR (NaCl, film): $\tilde{\nu}$ 3313 (w), 3268 (w), 3234 (w), 3189 (w), 3125 (w), 3064 (w), 3030 (w), 2980 (m), 2930 (s), 2857 (m), 1736 (m), 1701 (m), 1598 (m), 1552 (m), 1464 (m), 1312 (w), 1207 (m), 1145 (w), 1010 (w), 699 (w). Anal. Calcd for $C_{166}H_{200}N_8O_{19}S_2$: C, 74.52; H, 7.53; N, 4.19; S, 2.40. Found: C, 74.21; H, 7.54; N, 4.22; S, 2.26; ESI-MS (m/z): 1166 $[\mathbf{2}]^{++}$; mp: 89.5–91.5 °C.

*4.1.3.3. Compound **3**.* The resulting reddish solid residue was purified by column chromatography (*n*-hexane/ethyl acetate=2:1) to afford **3** (tosylate salt) as red solid compound (10%). ^{1}H NMR (C_6D_6, 300 MHz): δ 9.32 and 9.31 (6H, 2 br s), 8.21 (6H, d, J=8.1 Hz), 8.0–7.9 (12H, m), 7.72 (6H, s), 7.6 (2H, br s), 7.52 (6H, d, J=7.5 Hz), 7.39 (6H, d, J=7.2 Hz), 7.3–7.1 (12H, m), 7.04 (2H, br d), 6.96 (6H, d, J=7.2 Hz), 6.91 (3H, br t), 6.87 (2H, br d), 5.19 (1H, s), 5.09 (1H, s), 4.62 (6H, d, J=14.7 Hz), 4.2–4.1 (4H, m), 4–3.7 (19H, m), 3.52 (6H, d, J=14.7 Hz), 2.1 (2H, br s), 2.04 (6H, s), 2.0 (6H, br s), 1.81 (27H, s), 1.7–1.0 (26H, m); ^{13}C NMR (C_6D_6, 75 MHz): δ 176.8, 172.5, 152.4, 143.6, 142.5, 140.2, 139.9, 138.7 (2 resonances), 133.7, 133.1, 131.9, 129.1, 128.8, 128.6, 128.5, 128.3, 127.2, 126.7, 126.0, 124.0, 121.2, 117.5, 116.3, 77.2, 73.3, 65.3, 65.2, 61.2, 60.4, 58.4, 57.1, 53.0, 34.4, 31.8, 31.6, 31.3, 31.0, 30.7, 30.4, 30.1, 30.0, 29.6, 29.5, 29.4, 29.2, 28.9, 28.5, 28.3, 26.5, 26.0, 25.8, 22.6, 21.3, 14.1. Anal. Calcd for $C_{178}H_{224}N_8O_{19}S_2$: C, 75.18; H, 7.94; N, 3.94; S, 2.26. Found: C, 75.31; H, 8.04; N, 4.12; S, 2.14; ESI-MS (m/z): 1250 $[\mathbf{3}]^{++}$; mp: 92–94 °C.

4.2. Absorption and luminescence spectra

Measurements were carried out at room temperature (ca. 295 K) on air-equilibrated CH_2Cl_2 (Merck Uvasol™) solutions in the concentration range from 0.05 to 0.2 mM. UV–vis absorption and luminescence spectra were recorded with a Perkin–Elmer λ40 spectrophotometer and a LS50B spectrofluorimeter, respectively. For the luminescence spectra, excitation was performed at the wavelength of the absorption maximum. The experimental errors are as follows: wavelength values, ±1 nm; molar absorption coefficients, ±10%.

4.3. Electrochemical measurements

Cyclic voltammetric (CV) and differential pulse voltammetric (DPV) experiments were carried out in argon-purged CH_3CN or CH_2Cl_2 (Romil Hi-Dry™) with an Autolab 30 multipurpose instrument interfaced to a PC. The working electrode was a glassy carbon electrode (Amel; 0.07 cm^2); its surface was routinely polished with a 0.3 μm alumina-water slurry on a felt surface, immediately prior to use. In all cases, the counter electrode was a Pt wire, separated from the solution by a frit, an Ag wire was employed as a quasi-reference electrode and ferrocene was present as an internal standard ($E_{1/2}$=+0.395 and +0.460 V vs SCE in CH_3CN and in CH_2Cl_2, respectively). The concentration of the compounds examined was 0.5 mM; 50 mM tetraethylammonium hexafluorophosphate (in CH_3CN) or tetrabutylammonium hexafluorophosphate (in CH_2Cl_2) was added as supporting electrolyte. Cyclic voltammograms were obtained at sweep rates varying from 0.02 to 5 V s^{-1}. The DPV experiments were performed with a scan rate of 20 or 4 mV s^{-1} (pulse height 75 and 10 mV, respectively) and a duration of 40 ms. The IR compensation implemented within the Autolab 30 was used and every effort was made throughout the experiments in order to minimize the resistance of the solution. In any instance, the full electrochemical reversibility of the voltammetric wave of ferrocene was taken as an indicator of the absence of uncompensated resistance effects. The experimental error on the potential values was ±10 mV.

Acknowledgements

Financial support from MIUR (PRIN 2006034123), MAE (DGPCC), Regione Emilia-Romagna (NANOFABER) and the Universities of Bologna and Parma is gratefully acknowledged. The authors thank the Centro Interdipartimentale di Misure 'G. Casnati' of the University of Parma for NMR measurements.

References and notes

1. Balzani, V.; Credi, A.; Venturi, M. *Molecular Devices and Machines—Concepts and Perspectives for the Nanoworld*, 2nd ed.; Wiley-VCH: Weinheim, 2008.
2. Kay, E. R.; Leigh, D. A.; Zerbetto, F. *Angew. Chem., Int. Ed.* **2007**, *46*, 72–191.
3. Browne, W. R.; Feringa, B. L. *Nat. Nanotechnol.* **2006**, *1*, 25–35.
4. *Molecular Catenanes, Rotaxanes and Knots*; Sauvage, J. P., Dietrich-Buchecker, C., Eds.; Wiley-VCH: Weinheim, 1999.
5. Fyfe, M. C. T.; Stoddart, J. F. *Acc. Chem. Res.* **1997**, *30*, 393–401.
6. Philp, D.; Stoddart, J. F. *Angew. Chem., Int. Ed.* **1996**, *35*, 1155–1196.
7. Badjic, J. D.; Nelson, A.; Cantrill, S. J.; Turnbull, W. B.; Stoddart, J. F. *Acc. Chem. Res.* **2005**, *38*, 723–732.
8. Amabilino, D. B.; Stoddart, J. F. *Chem. Rev.* **1995**, *95*, 2725–2828.
9. Nepogodiev, S. A.; Stoddart, J. F. *Chem. Rev.* **1998**, *98*, 1959–1976.
10. Raymo, F. M.; Stoddart, J. F. *Chem. Rev.* **1999**, *99*, 1643–1663.
11. Cantrill, S. J.; Chichak, K. S.; Peters, A. J.; Stoddart, J. F. *Acc. Chem. Res.* **2005**, *38*, 1–9.
12. Balzani, V.; Credi, A.; Raymo, F. M.; Stoddart, J. F. *Angew. Chem., Int. Ed.* **2000**, *39*, 3349–3391.
13. Pease, A. R.; Jeppesen, J. O.; Stoddart, J. F.; Luo, Y.; Collier, C. P.; Heath, J. R. *Acc. Chem. Res.* **2001**, *34*, 433–444.
14. Credi, A.; Tian, H. *Adv. Funct. Mater.* **2007**, *17*, 679–682.
15. Anelli, P. L.; Spencer, N.; Stoddart, J. F. *J. Am. Chem. Soc.* **1991**, *113*, 5131–5133.
16. Bissell, R. A.; Córdova, E.; Kaifer, A. E.; Stoddart, J. F. *Nature* **1994**, *369*, 133–137.
17. Nygaard, S.; Leung, K. C.-F.; Aprahamian, I.; Ikeda, T.; Saha, S.; Laursen, B. W.; Kim, S.-Y.; Hansen, S. W.; Stein, P. C.; Flood, A. H.; Stoddart, J. F.; Jeppesen, J. O. *J. Am. Chem. Soc.* **2007**, *129*, 960–967.
18. Saha, S.; Flood, A. H.; Stoddart, J. F.; Impellizzeri, S.; Silvi, S.; Venturi, M.; Credi, A. *J. Am. Chem. Soc.* **2007**, *129*, 12159–12171.
19. Durola, F.; Sauvage, J.-P. *Angew. Chem., Int. Ed.* **2007**, *46*, 3537–3540.
20. Crowley, J. D.; Leigh, D. A.; Lusby, P. J.; McBurney, R. T.; Perret-Aebi, L.-E.; Petzold, C.; Slawin, A. M. Z.; Symes, M. D. *J. Am. Chem. Soc.* **2007**, *129*, 15085–15090.
21. Vella, S. J.; Tiburcio, J.; Loeb, S. J. *Chem. Commun.* **2007**, 4752–4754.
22. Balzani, V.; Clemente-León, M.; Credi, A.; Ferrer, B.; Venturi, M.; Flood, A. H.; Stoddart, J. F. *Proc. Natl. Acad. Sci. U.S.A.* **2006**, *103*, 1178–1183.
23. Qu, D.-H.; Wang, Q.-C.; Ma, X.; Tian, H. *Chem.—Eur. J.* **2005**, *11*, 5929–5937.
24. Arduini, A.; Ferdani, R.; Pochini, A.; Secchi, A.; Ugozzoli, F. *Angew. Chem., Int. Ed.* **2000**, *39*, 3453–3456.
25. Arduini, A.; Calzavacca, F.; Pochini, A.; Secchi, A. *Chem.—Eur. J.* **2003**, *9*, 793–799.
26. Arduini, A.; Ciesa, F.; Fragassi, M.; Pochini, A.; Secchi, A. *Angew. Chem., Int. Ed.* **2005**, *44*, 278–281.
27. Ugozzoli, F.; Massera, C.; Arduini, A.; Pochini, A.; Secchi, A. *CrystEngComm* **2004**, *6*, 227–232.
28. Credi, A.; Dumas, S.; Silvi, S.; Venturi, M.; Arduini, A.; Pochini, A.; Secchi, A. *J. Org. Chem.* **2004**, *69*, 5881–5887.
29. Arduini, A.; Credi, A.; Faimani, G.; Massera, C.; Pochini, A.; Secchi, A.; Semeraro, M.; Silvi, S.; Ugozzoli, F. *Chem.—Eur J.* **2008**, *14*, 98–106.
30. Hamilton, D. G.; Montalti, M.; Prodi, L.; Fontani, M.; Zanello, P.; Sanders, J. K. M. *Chem.—Eur. J.* **2000**, *6*, 608–617.
31. Hush, N. S. *Prog. Inorg. Chem.* **1967**, *8*, 391–444.
32. Creutz, C. *Prog. Inorg. Chem.* **1983**, *30*, 1–73.
33. Anelli, P. L.; Ashton, P. R.; Ballardini, R.; Balzani, V.; Delgado, M.; Gandolfi, M. T.; Goodnow, T. T.; Kaifer, A. E.; Philp, D.; Pietraszkiewicz, M.; Prodi, L.; Reddington, M. V.; Slawin, A. M. Z.; Spencer, N.; Stoddart, J. F.; Vicent, C.; Williams, D. J. *J. Am. Chem. Soc.* **1992**, *114*, 193–218.
34. Ashton, P. R.; Ballardini, R.; Balzani, V.; Credi, A.; Gandolfi, M. T.; Menzer, S.; Peréz-García, L.; Prodi, L.; Stoddart, J. F.; Venturi, M.; White, A. J. P.; Williams, D. J. *J. Am. Chem. Soc.* **1995**, *117*, 11171–11197.
35. Raymo, F. M.; Bartberger, M. D.; Houk, K. N.; Stoddart, J. F. *J. Am. Chem. Soc.* **2001**, *123*, 9264–9267.
36. Ishow, E.; Credi, A.; Balzani, V.; Spadola, F.; Mandolini, L. *Chem.—Eur. J.* **1999**, *5*, 984–989.
37. Balzani, V.; Credi, A.; Venturi, M. *Stimulating Concepts in Chemistry*; Vögtle, F., Stoddart, J. F., Shibasaki, M., Eds.; Wiley-VCH: Weinheim, 2000; pp 255–266.
38. Monk, P. M. S. *The Viologens: Physicochemical Properties, Synthesis and Applications of the Salts of 4,4′-Bipyridine*; Wiley: Chichester, UK, 1998.
39. Ballardini, R.; Credi, A.; Gandolfi, M. T.; Giansante, C.; Marconi, G.; Silvi, S.; Venturi, M. *Inorg. Chim. Acta* **2007**, *360*, 1072–1082.
40. Bard, A. J.; Faulkner, L. R. *Electrochemical Methods—Fundamentals and Applications*, 2nd ed.; Wiley: New York, NY, 2001.
41. Kaifer, A. E.; Gómez-Kaifer, M. *Supramolecular Electrochemistry*; Wiley-VCH: Weinheim, 1999.
42. Cardona, C. M.; Mendoza, S.; Kaifer, A. E. *Chem. Soc. Rev.* **2000**, *29*, 37–42.
43. Ong, W.; Gómez -Kaifer, M.; Kaifer, A. E. *Chem. Commun.* **2004**, 1677–1683.
44. Ashton, P. R.; Ballardini, R.; Balzani, V.; Belohradsky, M.; Gandolfi, M. T.; Philp, D.; Prodi, L.; Raymo, F. M.; Reddington, M. V.; Spencer, N.; Stoddart, J. F.; Venturi, M.; Williams, D. J. *J. Am. Chem. Soc.* **1996**, *118*, 4931–4951.
45. Asakawa, M.; Ashton, P. R.; Ballardini, R.; Balzani, V.; Belohradsky, M.; Gandolfi, M. T.; Kocian, O.; Prodi, L.; Raymo, F. M.; Stoddart, J. F.; Venturi, M. *J. Am. Chem. Soc.* **1997**, *119*, 302–310.
46. Ashton, P. R.; Ballardini, R.; Balzani, V.; Credi, A.; Dress, K. R.; Ishow, E.; Kleverlaan, C. J.; Kocian, O.; Preece, J. A.; Spencer, N.; Stoddart, J. F.; Venturi, M.; Wenger, S. *Chem.—Eur. J.* **2000**, *6*, 3558–3574.
47. Benniston, A. C.; Harriman, A.; Li, P.; Rostron, J. P.; Harrington, R. W.; Clegg, W. *Chem.—Eur. J.* **2007**, *13*, 7838–7851.
48. Gonzàlez, J. J.; Ferdani, R.; Albertini, E.; Blasco, J. M.; Arduini, A.; Pochini, A.; Prados, P.; de Mendoza, J. *Chem.—Eur. J.* **2000**, *6*, 73–80.
49. Bradshaw, J. S.; Krakowiak, K. E.; Lindh, G. C.; Izatt, R. M. *Tetrahedron* **1987**, *43*, 4271–4276.
50. Chang, S.-Y.; Choi, J. S.; Jeong, K.-S. *Chem.—Eur. J.* **2001**, *7*, 2687–2697.
51. Ballot, S.; Noiret, N. *Tetrahedron Lett.* **2003**, *44*, 8811–8814.